RB March 1943

Lockheed 6-35/7

NATIONAL ADVISORY COMMITTEE FOR AERONAUTICS

WARTIME REPORT

ORIGINALLY ISSUED

XC-35 GUST RESEARCH PROJECT

PRELIMINARY ANALYSIS OF THE LATERAL DISTRIBUTION OF GUST VELOCITY ALONG THE SPAN OF AN AIRPLANE

By A. I. Moskovitz

NACA

WASHINGTON

NATIONAL ADVISORY COMMITTEE FOR AERONAUTICS

RESTRICTED BULLETIN

XC-35 GUST RESEARCH PROJECT

PRELIMINARY ANALYSIS OF THE LATERAL DISTRIBUTION OF GUST VELOCITY ALONG THE SPAN OF AN AIRPLANE

By A. I. Moskovitz

SUMMARY

Measurements of the lateral distribution of effective gust velocity along the span of the XC-35 airplane were made during the spring and summer of 1941 under a wide variety of weather conditions at altitudes up to 34,000 feet. The lateral distributions of effective gust velocity were derived from the measurement of the pressure coefficient at the 25-percent-chord position at four stations along the span of the airplane by means of orifice installations. The lateral distributions assumed many configurations and were consequently divided into six standard shapes.

The "triangular" gust (called triangular because the gust velocity is a maximum near the center of the wing and decreases linearly toward the wing tips) was the most frequently encountered shape and included about 84 percent of all the data. The average lateral gust gradient distance for the XC-35 airplane was found to be 9 chord lengths, which is in good agreement with the longitudinal gust gradient distance obtained with the same airplane. Thus the "design" gust of 30K feet per second, where K is the effective gust factor, can be considered to be a triangular gust with longitudinal and lateral gradient distances of 9 chord lengths. The bending moment at the wing root for the design triangular gust is 6 percent lower than that produced by the design rectangular gust used in the present design of wings for gust loads. The most probable value of the average effective gust velocity obtained for the critical "unsymmetrical" gust (called unsymmetrical because the gust velocity decreases linearly along the span from a maximum at one wing tip to a minimum at the other)

is 23K feet per second, which agrees with similar results previously obtained.

INTRODUCTION

In past gust research investigations involving atmospheric turbulence at altitudes greater than a few hundred feet, the assumption that the distribution of gust velocity along the span of the airplane was known (see references 1 and 2) had to be made because of the lack of detailed information. For work pertaining to the symmetrical gust loading of airplane wings, the gust velocity was assumed to be constant along the entire span (see reference 1) and, for unsymmetrical gust loading, the gust velocity was assummed to vary linearly along the span from a maximum gust velocity at one wing tip to a minimum at the other wing tip (see reference 3). On the basis of these assumptions, the calculated stresses for the wing structure were conservative.

Information pertaining to the lateral distribution of gust velocity is highly desirable for a more accurate solution of both symmetrical and unsymmetrical gust-load problems and, if available, would aid in the design of airplane wings. This paper presents data on the lateral distribution of gust velocity along the span of the XC-35 airplane. These data were obtained by measuring simultaneously the resultant pressure at four stations along the span of the airplane and the dynamic pressure. The data were accumulated during the first stages of the gust research program on the XC-35 airplane in the summer of 1941. The results were considered insufficient for a final analysis but were thought to be of enough interest to warrant presentation.

METHOD AND APPARATUS

The Lockheed XC-35 airplane, which is described in reference 4, was used in the investigation reported herein. For convenience, the pertinent characteristics of the airplane are listed as follows:

Gross weight, pounds	11,139
Wing area, square feet	458.3
Wing loading, pounds per square foot	24.3
Span, feet	55
Mean aerodynamic chord, feet	9.23
Center of gravity, percent mean aerodynamic chord	24.4
Tail length, feet	25.5
Elevator area, square feet	31.3
Stabilizer area, square feet	65.4
Aspect ratio	6.6
Taper ratio	3:1

The airplane was flown in level flight and, whenever rough air was encountered, the resultant pressure at four stations along the span of the wing and the dynamic pressure were recorded. A complete description of the method used in the tests is given in reference 4.

The evaluation of the dynamic and resultant pressure records to obtain values of gust velocity is based on the following assumptions and relations:

(1) The pressure coefficient P is a linear function of the lift coefficient and consequently of the angle of attack (see reference 5):

$$P = P_1 + K_1 C_L = P_2 + K_2 \alpha$$

where

P pressure coefficient (p/q)

P resultant pressure

q dynamic pressure

K_1 slope of curve of P against C_L

K_2 slope of curve of P against α

C_L lift coefficient

α angle of attack

and the subscripts have the following significance:

1 at zero value of C_L

2 at zero value of α

(2) The relation between the pressure coefficient P and the angle of attack is unaffected by the rate of change of angle of attack.

(3) The gust velocity is normal to the flight path of the airplane.

(4) The airplane is in steady flight prior to and during the traverse of the gust.

(5) The local angle of attack at any point along the span of an airplane is independent of the load distribution.

(6) The ailerons are not displaced during the traverse of a gust.

On the basis of these assumptions, the local value of effective gust velocity can be obtained from measurements of P, because

$$P = P_2 + K_2\alpha$$

and

$$\Delta P = K_2\Delta\alpha = K_2 \frac{U_{e_2}}{V_i} = K_2 \frac{U_{et_2}}{V_t}$$

where

ΔP increment of pressure coefficient

$\Delta\alpha$ increment of angle of attack

U_e effective gust velocity, feet per second (see reference 6)

U_{et} true effective gust velocity, feet per second $\left(U_e \sqrt{\rho_0/\rho}\right)$

ρ mass density of air at altitude

ρ_o mass density of air at sea level

V_i indicated airspeed

V_t true airspeed

and the subscript o, used with U_e and U_{et}, represents values obtained from pressure records.

For the evaluation of the data, the value of K_2 was determined by measuring the pressure coefficient P at the various stations along the wing of the airplane and the angle of attack of the airplane throughout the steady flight range. The records obtained in rough air were evaluated by determining the magnitude of the changes in pressure coefficient from steady conditions.

Comparison of the method of evaluating the data from pressure records to obtain gust velocities and the method (reference 4) of obtaining effective gust velocities from accelerometer and airspeed data indicates that the two methods yield the same results. The average gust velocity along the span should be equal, therefore, to the effective gust velocity obtained from accelerometer data. An important difference in the methods of evaluation of the two types of data, however, is that, for the accelerometer data, the increments of acceleration are taken from an arbitrary datum line 1 g (reference 4); whereas, for the pressure data, the increments of pressure are taken from the steady value of pressure just prior to the entry into a gust.

Although the motion of the airplane under the action of the gust is neglected, the gust velocity obtained from pressure records is reduced from the truevalue by the pitching motion of the airplane, which tends to alleviate the effect of the gust. Since no measure of the motion of the airplane is obtained from the pressure measurements, as is obtained from the acceleration data, it is not practical at this time to obtain a "true" gust velocity as is done for the acceleration data in references 1 and 4.

The pressure measurements along the wing were made at locations shown in figure 1. The resultant pressures were obtained by installing orifices in the upper and lower surfaces of the wing at the 25-percent-chord position at each of the four stations, and each pair of orifices at each station were connected to the same pressure capsule. The

orifices on the wing were so located that they would not be affected by the propeller slipstream and yet would have optimum spanwise spacing. The chordwise position of the orifices at the 25-percent-chord point was selected to insure that the variation in pressure would be within the range of available pressure capsules.

The following instruments were used to record the desired data:

NACA airspeed recorders

(a) Two with two pressure capsules each to measure resultant pressure at each station

(b) One with one pressure capsule to obtain a record of the dynamic pressure by suitable connections to the pitot-static tube

NACA timer (1-second interval)

NACA control-position recorder to record the displacement of the ailerons

All instruments were fitted with magazine film drums that have a capacity of 20 feet of film. At a film speed of 1/8 inch per second, approximately 30 minutes of records could be obtained.

TESTS

Records of resultant pressures at the four stations and of dynamic pressure were obtained during traverses through cumuliform clouds and turbulent air at altitudes up to 34,000 feet. A more complete description of the tests to obtain the required data is contained in reference 4. Although there were 16 flights, only 14 were satisfactory because one flight was too smooth to warrant evaluation and because, in another flight, one of the records of resultant pressure was spoiled by a leak in the orifice installation.

RESULTS

The records of resultant and dynamic pressure were evaluated to obtain, for each gust, the local value of

effective and true effective gust velocities at each of the four stations. The data for each gust were combined to obtain the lateral gust distribution. Because the distribution of gust velocity along the span may assume numerous shapes, which tend to complicate the presentation of the data, all the various distributions were reduced to six simple configurations. The "standard" distributions and their assigned names are shown in figure 2, together with the variations that were considered similar. The frequency of occurrence of each gust shape has been included in figure 2. In order to investigate the effect of power not accounted for in the calibration of the orifice installation, a count of the various types that can be right- or left-handed was made and, as might be expected, the frequency was found to be the same for each hand; this phase of the question was therefore disregarded and all the data for a given type of distribution were combined.

The gust shapes in figure 2 were simplified to obtain, whenever possible, the average value of effective gust velocity along the span $(U_{e_o})_{av}$ and the value of the maximum or minimum effective-gust-velocity increments $\pm\Delta U_{e_o}$, which represent deviations from the average. Figure 3 shows $\pm\Delta U_{e_o}$ as a function of $(U_{e_o})_{av}$ for five gust shapes. By use of figure 3, a gust can be specified, within the accuracy of the data, by the shape, the average effective gust velocity, and the effective-gust-velocity increment.

If linearity of the lateral variation of gust velocity is assumed, the variation along the span can be used to determine the lateral gust gradient distance H_{s_o} by extrapolating the distribution of gust velocity in the spanwise direction to zero. The lateral gust gradient distance is, then, the distance from the maximum gust velocity measured at one of the inboard stations to the point of zero gust velocity, as shown in figure 4. This method of evaluating lateral gust gradient distance fails if the local gust velocity at either tip station is equal to or greater than the gust velocity at its corresponding inboard station. If the method is applied to the six lateral gust-velocity distributions in figure 2, the triangular and second trapezoidal gusts yield two values of H_{s_o}, the first trapezoidal and the double triangular gust yield one value of H_{s_o}, and the rectangular and unsymmetrical gusts yield no values of H_{s_o}.

The lateral gust distributions were evaluated as described to obtain the lateral gust gradient distance H_{s_o}. In order to present the data in a form similar to that of figure 1 of reference 4, the values of the true gust velocity U_t obtained from the data of reference 4 have been plotted in figure 5 as a function of the lateral gust gradient distance H_{s_o}. For ranges of true gust velocity U_t in figure 5, the average values of the lateral gust gradient distance H_{s_o} converted to chord lengths were calculated and the results plotted in figure 6. This figure presents the data in a form comparable with that of figure 3 of reference 4 for the longitudinal gust gradient distances.

PRECISION

The precision of the recorded data is estimated to be within the following limits:

Airspeed, miles per hour	±4
Time, seconds	±0.05
Dynamic pressure, pounds per square foot	±2.0
Total pressure, pounds per square foot	±2.0
Average effective gust velocity $(U_{e_o})_{av}$, feet per second	±4.0

As previously noted, the value of effective gust velocity determined by means of the formula for the sharp-edge gust is essentially the same as the value of the average gust velocity over the span evaluated from the pressure data. A comparison of the values of the average gust velocity for each gust where both methods of evaluation were used appeared to be the best way to show the precision of the results. For this purpose, the average value of the effective gust velocity $(U_{e_o})_{av}$ for each gust was plotted against the effective gust velocity U_e for 25 percent of the data, as shown in figure 7. Inspection of all the available data indicated that, for 80 percent of the cases, the gust velocities agreed within the instrumental error (±4 fps). For the remainder of the data all except one of the values of the average effective gust velocity $(U_{e_o})_{av}$ indicated discrepancies of less than ±10 feet per second. The one outstanding point shows a discrepancy of 17 feet per second.

The discrepancies greater than ±4 feet per second can be ascribed to the different bases on which the records are evaluated, as previously mentioned. As an example, the gust velocities corresponding to the discrepancy of 17 feet per second were 48 feet per second for the pressure data and 31 feet per second for the accelerometer and airspeed data. If the acceleration peak corresponding to this gust is evaluated by use of the value of acceleration just prior to the peak as the datum instead of the 1 g line, the effective gust velocity so obtained is 44 feet per second, which is in agreement with the value from the pressure data within the instrumental error. It is reasonable to assume that, if the method of evaluating effective gust velocities were modified in this way, all the data would agree within the instrumental error.

The position of the peak of the lateral gust-velocity distribution between the two inboard stations is not known because of the limitations of the orifice installation. A possible error will therefore be present in the value of the effective-gust-velocity increment $\pm\Delta U_{e_o}$ and the average effective gust velocity $(U_{e_o})_{av}$ if the actual gust shapes deviate radically from those assumed. The magnitude of the error is unknown but can be considered equal to the discrepancies between U_e and $(U_{e_o})_{av}$. (See fig. 7.)

The lateral gust gradient distances are estimated to be accurate to within ±20 percent. The possible errors are known to be large, particularly for long gradient distances because a small error in gust velocity can cause a large error in the gust gradient distance. An additional source of error is the fact that the actual peak of the gust may be between stations rather than at a station as assumed.

DISCUSSION

The data on the frequency with which the various types of gust were encountered (see fig. 2) indicate that the rectangular and first trapezoidal gust shapes were rare and therefore do not appear worthy of consideration in the design of wings for gust loads. The triangular, the double triangular, and the second trapezoidal gusts, which are condidered in the same category in the present report, represent 84 percent of all the gusts evaluated. Although

the shapes of the double triangular and the triangular gusts are not alike, they can be combined into one group since both produce approximately the same amount of bending moment at the root chord and very little rolling motion as compared with the unsymmetrical gust shape. Inasmuch as the gust velocity at an outboard station is greater than the gust velocity at an adjacent inboard station, the rolling motion due to the double triangular gust will be decreased although the wing bending stresses at the inboard station will increase, which indicates that the double triangular gust cannot be included with the unsymmetrical gust. The unsymmetrical gust, which is the next most frequent shape encountered, is of interest since this type of gust would cause rolling motions of the airplane. If the same relative distribution of gust shape is assumed to hold for all gust data, the gust data obtained by means of V-G recorders on transport airlines (reference 7) should conform to this distribution.

The fairest comparison of the average intensity of the various gust shapes would be on the basis of the intensities of gusts occurring with the same frequency. Frequency curves were plotted, therefore, and from these curves corresponding values of the gust intensities at different frequencies were noted. The results of this analysis are given in figure 8 where the values of corresponding intensities have been plotted for the unsymmetrical gust and the rectangular gust combined with the first trapezoidal gust as a function of the intensity of the triangular gust, which includes the triangular, the double triangular, and the second trapezoidal gusts. Figure 8 indicates that, as might be expected, the relative intensities of the various gust shapes are in the same order as the frequencies of occurrence. If the triangular gust is assumed to have an average intensity of 32.1 feet per second (30K fps where K is the effective gust factor, from reference 8), the corresponding intensity of the unsymmetrical gust would be 24.6 feet per second (23K fps) and the corresponding value of the rectangular gusts combined with the first trapezoidal gusts would be 11.3 feet per second (10.6K fps). Thus, the magnitude of the average intensities indicates, within the limits of these data, that the triangular and the unsymmetrical gust shapes represent the gusts which will probably apply critical loads to the wing of an airplane. It might be noted in connection with the unsymmetrical gust shape that the value of 23K feet per second is in good agreement with the value of 24 feet per second proposed in reference 3.

Inspection of the triangular gust shapes in figure 3 indicates that the gust-velocity increments attained a maximum value of about 9 feet per second for average gust velocities up to 20 feet per second but for the higher gust velocities the maximum values were about 4 to 7 feet per second. The data indicate, therefore, that the critical symmetrical gust with an average intensity of 30K feet per second (reference 8) would have a maximum value at the apex of 36K feet per second (near the center line) and would decrease linearly to a value of about 24K feet per second at each wing tip. This analysis is verified to some degree by inspection of the data presented in figure 3.

Figure 6 indicates that, for all gust intensities, the most probable value of the lateral gradient distance is 9 chord lengths. If this information is used, together with an average gust intensity of 30K feet per second, then the maximum intensity of the gust is 36K feet per second and decreases linearly to 24K feet per second at each wing tip for the XC-35 airplane. As shown by these data the design gust of 30K feet per second would be a triangular gust with longitudinal and lateral gradient distances of 9 chord lengths. The critical triangular gust would give a wing root bending moment that would be 6 percent lower than the present CAA design requirement for gust load given in reference 8.

In applying such data to airplanes of other sizes, a question arises as to whether the chord length or the airplane span is the better measure of lateral gust gradient distance. For conventional airplanes such as the XC-35 airplane (airplanes with geometrically similar plan forms) either measure is satisfactory. For unconventional airplanes with extreme values of aspect ratio, it would appear desirable to express the gust gradient distances in terms of the quantity that gives the largest load factor. Thus the gradient distance to be used would be about 9 chord lengths or about 1.25 span lengths. The amount of data available at the present time is insufficient to settle this question.

The data on unsymmetrical gusts in the present report agree with the data of reference 3 relative to the average gust intensity but indicate (fig. 3) that the effective-gust-velocity increment, corresponding to U_t in reference 3, is very conservative. The data show that the maximum effective-gust-velocity increment measured during the current tests was only ±9 feet per second as compared

with ±20 feet per second, the value suggested in reference 3.

CONCLUDING REMARKS

Additional data are required before any definite conclusions can be drawn regarding the magnitude and the freqency of the various gust shapes. On the basis of the information presented, which was obtained from flight tests, the following remarks appear in order.

The most probable lateral gust shape encountered in flight is triangular. The other gust shapes in order of their respective frequencies are the unsymmetrical and the rectangular combined with the first trapezoidal shapes.

If the magnitude of the average effective gust velocity for the critical triangular gust is considered to be 30K feet per second, where K is the effective gust factor, the average effective gust velocity for the critical unsymmetrical gust, based on the same frequency, would be 23K feet per second. This value is in good agreement with a similar value for the unsymmetrical gust previously obtained.

The lateral gust gradient distance is found to be 9 chord lengths, which agrees with the value for the longitudinal gust gradient distance obtained previously for the same airplane. Thus, the shape of the most probable critical gust encountered will be triangular with equal longitudinal and lateral gust gradient distances of 9 chord lengths and an average gust velocity of 30K feet per second (36K fps at the center of the wing decreasing linearly to 24K fps at each wing tip).

The maximum increment of effective gust velocity obtained in flight for the unsymmetrical gust was ±9 feet per second, which indicates that the value for effective-gust-velocity increment previously obtained is conservative as compared with the data herein presented.

Data on airplanes of different size and wing plan form similar to data reported herein are desirable in

order to compare the lateral gust-velocity distributions for the different size airplanes.

Langley Memorial Aeronautical Laboratory,
National Advisory Committee for Aeronautics,
Langley Field, Va.

REFERENCES

1. Donely, Philip: Effective Gust Structure at Low Altitudes as Determined from the Reactions of an Airplane. Rep. No. 692, NACA, 1940.

2. Rhode, Richard V.: Gust Loads on Airplanes. SAE Trans., vol. 32, 1937, pp. 81-83.

3. Rhode, Richard V., and Pearson, Henry A.: A Semi-Rational Criterion for Unsymmetrical Gust Loads. NACA A.R.R., Aug. 1941.

4. Flight Research Loads Section: XC-35 Gust Research Project Bulletin No. 6. Preliminary Analysis of Gust Measurements. NACA R.B., April 1942.

5. Jacobs, Eastman N., and Rhode, R. V.: Airfoil Section Characteristics as Applied to the Prediction of Air Forces and Their Distribution on Wings. Rep. No. 631, NACA, 1938.

6. Flight Research Loads Section: XC-35 Gust Research Project Bulletin No. 1 - Operations in Vicinity of Cold Front, May 23, 1941 - Evaluation of Maximum Gust Intensities. NACA A.R.R., Sept. 1941.

7. Walker, Walter G.: Gust Loads on Transport Airplanes. NACA R.B., July 1942.

8. Anon: Airplane Airworthiness. Pt. 04 of Civil Aero. Manual, CAA, U.S. Dept. Commerce, Feb. 1, 1941, sec. 04.2121.

BIBLIOGRAPHY

Flight Research Loads Section: XC-35 Gust Research Project Bulletin No. 2 - Operations in Vicinity of Cold Front, May 23, 1941 - Reactions of Pilot's Instruments. NACA A.R.R., Oct. 1941.

Flight Research Loads Section: XC-35 Gust Research Project Bulletin No. 3 - Operations in Cumulo-Nimbus and Cumulus Congestus Clouds on July 3, 1941 - Maximum Gust Intensities. NACA R.B., March 1942.

Flight Research Loads Section: XC-35 Gust Research Project - Operations in Cumulus Congestus Cloud on July 31, 1941 - Maximum Gust Intensities. NACA R.B., April 1942.

Flight Research Loads Section: XC-35 Gust Research Project Bulletin No. 5 - Operations near Cold Front on August 12, 1941 - Maximum Gust Intensities. NACA R.B., April 1942.

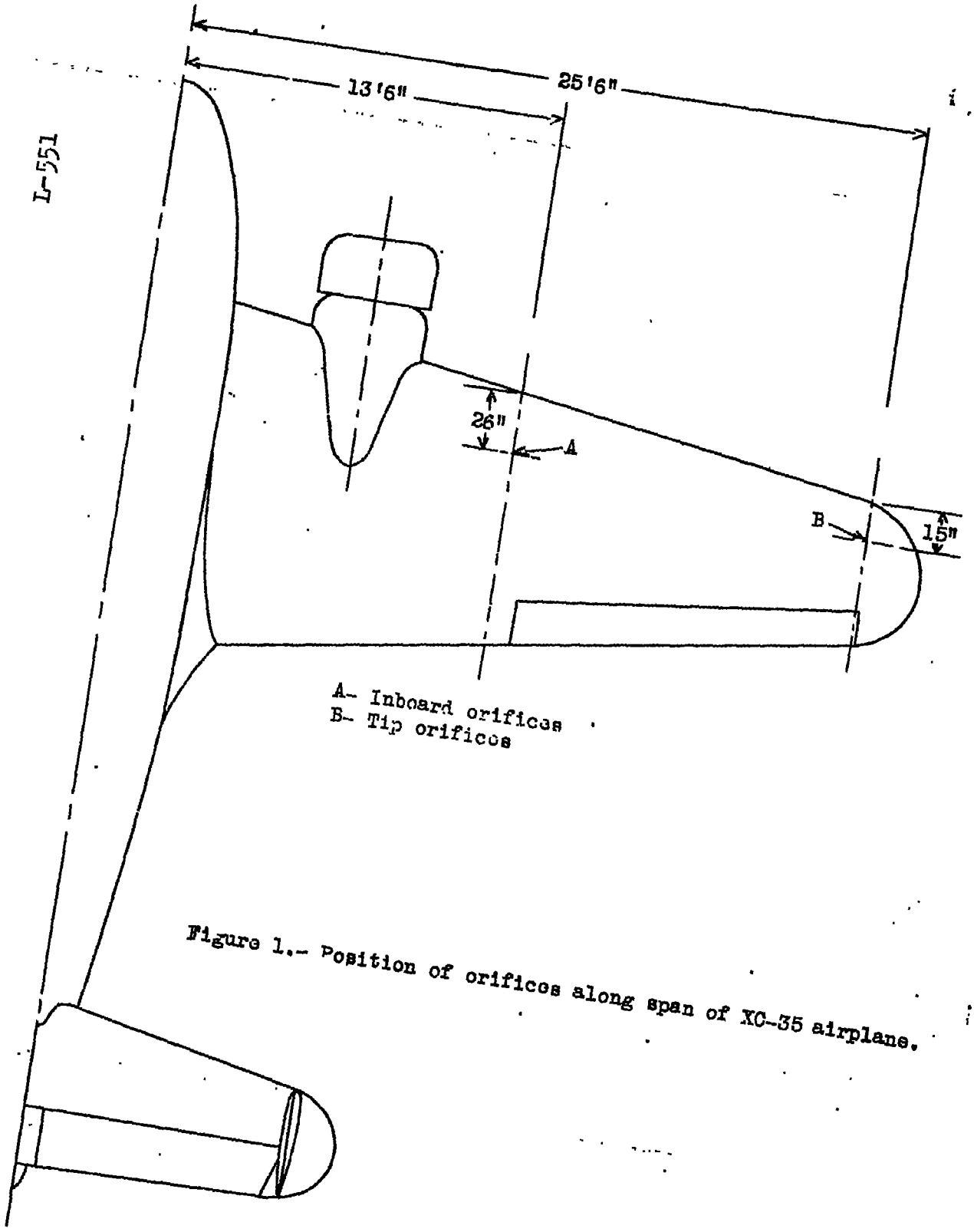

Figure 1.- Position of orifices along span of XC-35 airplane.

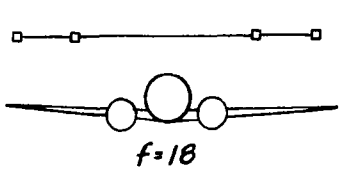

Rectangular

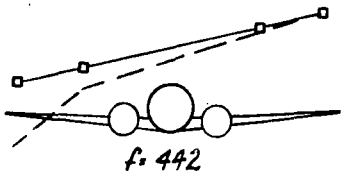

Unsymmetrical

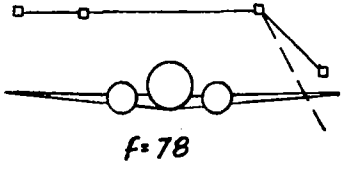

First trapezoidal

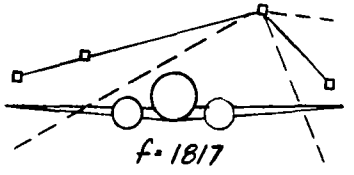

Triangular

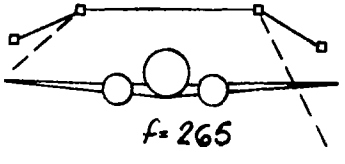

Second trapezoidal

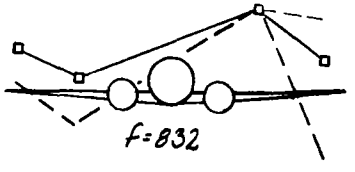

Double triangular

— "Standard" distribution
-- Possible deviation from the "standard"
▫ Position where local gust velocity U_{e_o} is measured

Figure 2.— Spanwise gust distributions and frequency of occurrence f for each type.

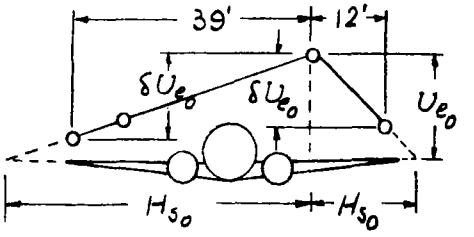

Ideal triangular distribution

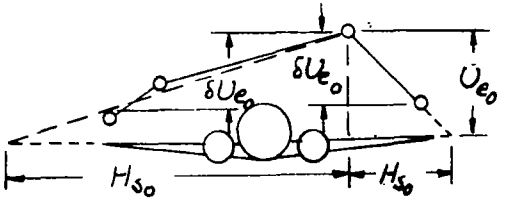

Triangular distribution

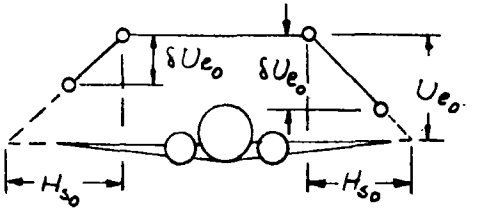

Trapezoidal distribution

o Local value of effective gust velocity U_{e_o} at selected stations

Figure 4.- Graphic method for evaluating lateral gust gradient distance H_{s_o} from the local values of the effective gust velocity U_{e_o} along the span of an airplane. (δ is the difference between any two values of U_{e_o}.)

$$H_{s_o} = \frac{U_{e_o} \times 39}{\delta U_{e_o}} \qquad H_{s_o} = \frac{U_{e_o} \times 12}{\delta U_{e_o}}$$

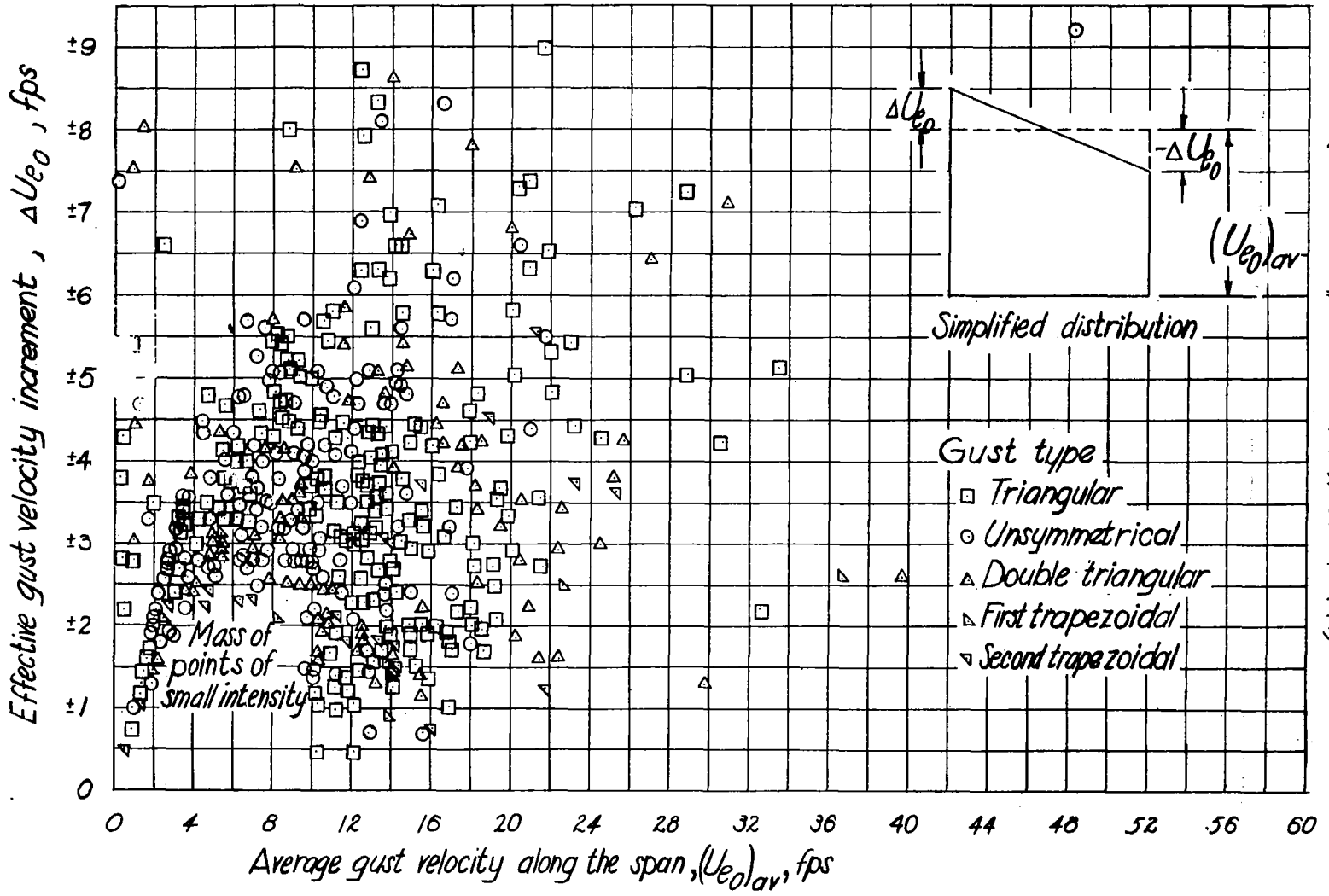

Figure 3.— Effective gust velocity increment $\pm \Delta U_{e_0}$ as a function of the average effective gust velocity $(U_{e_0})_{av}$ for five types of gust shape.

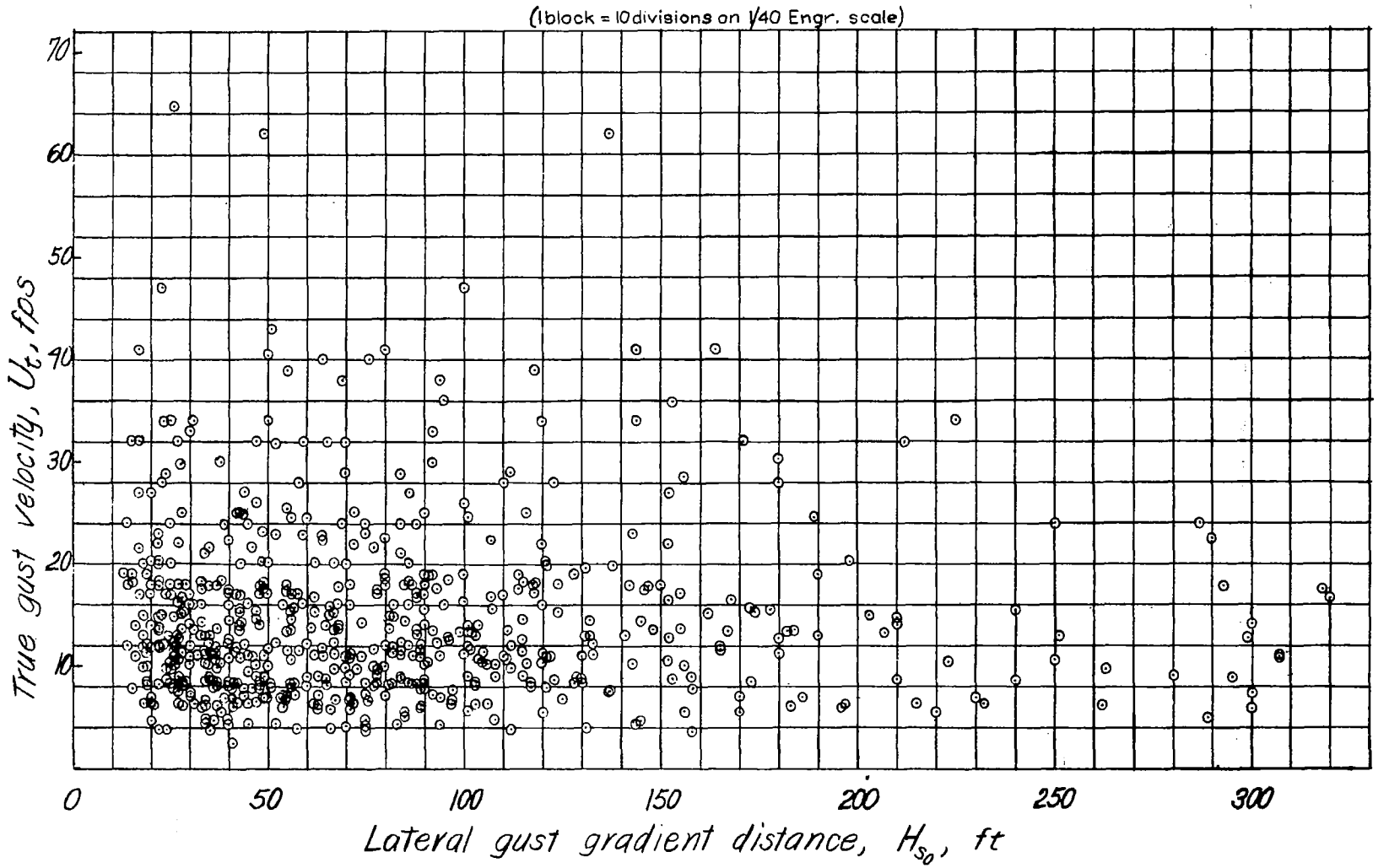

Figure 5.–True gust velocity as a function of lateral gust gradient distance. (True gust velocity data from reference 4.)

L-551

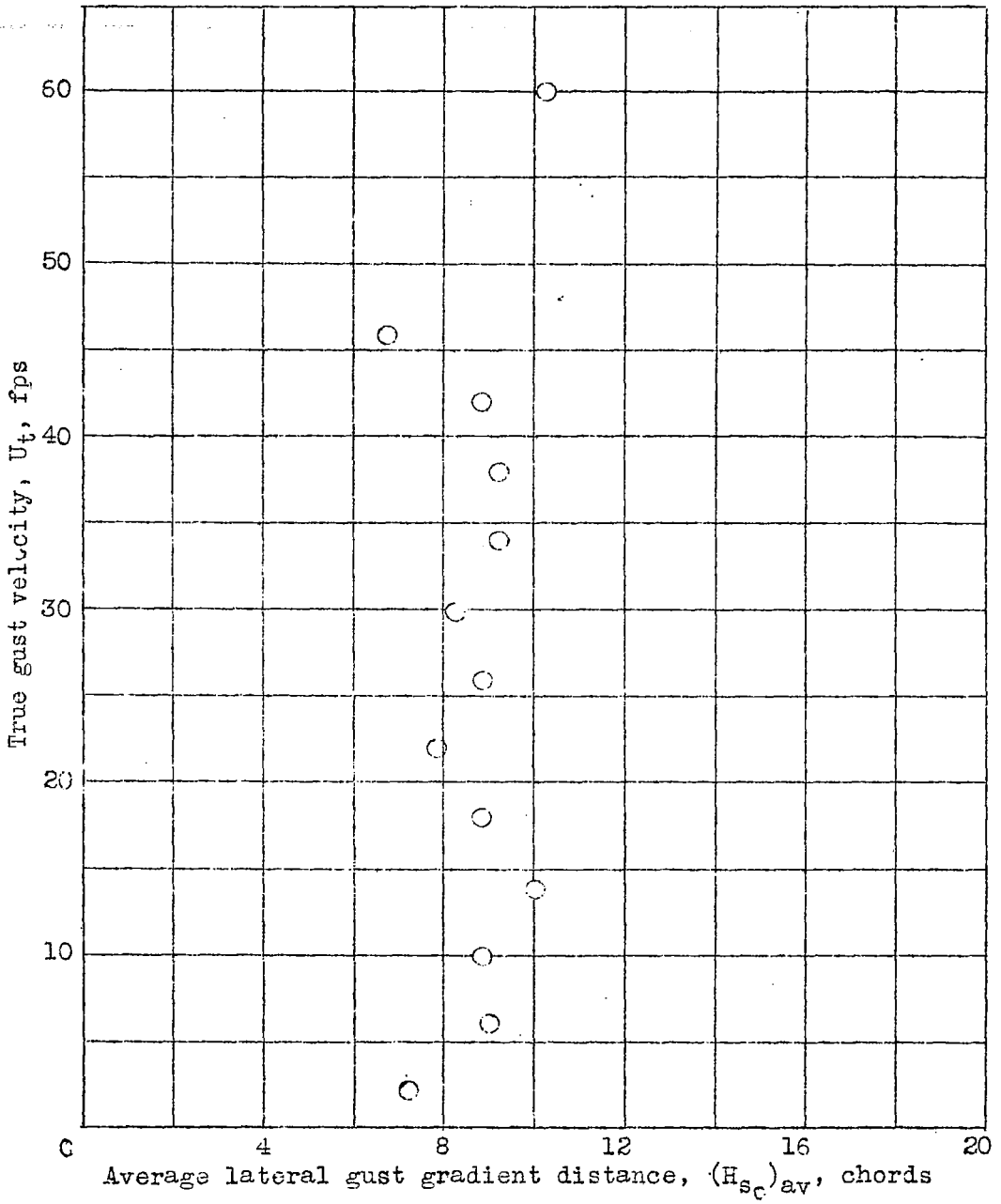

Figure 6.- Variation of the true gust velocity with average lateral gust gradient distance.

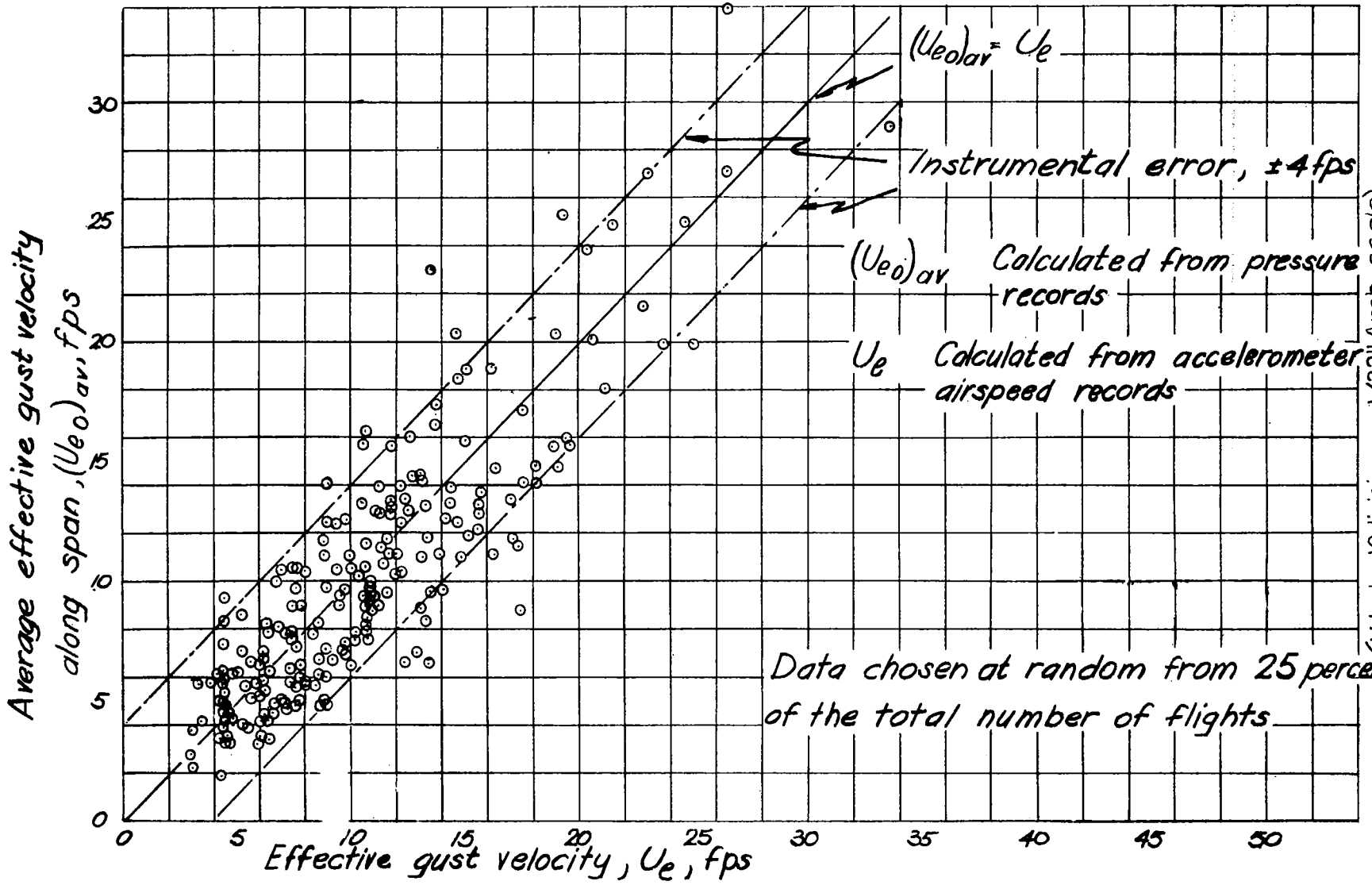

NACA

(1 block = 10 divisions on 1/32" Arch scale)

Fig. 7

Figure 7.- Comparison of the effective gust velocity with the average effective gust velocity along the span of the XC-35 airplane.

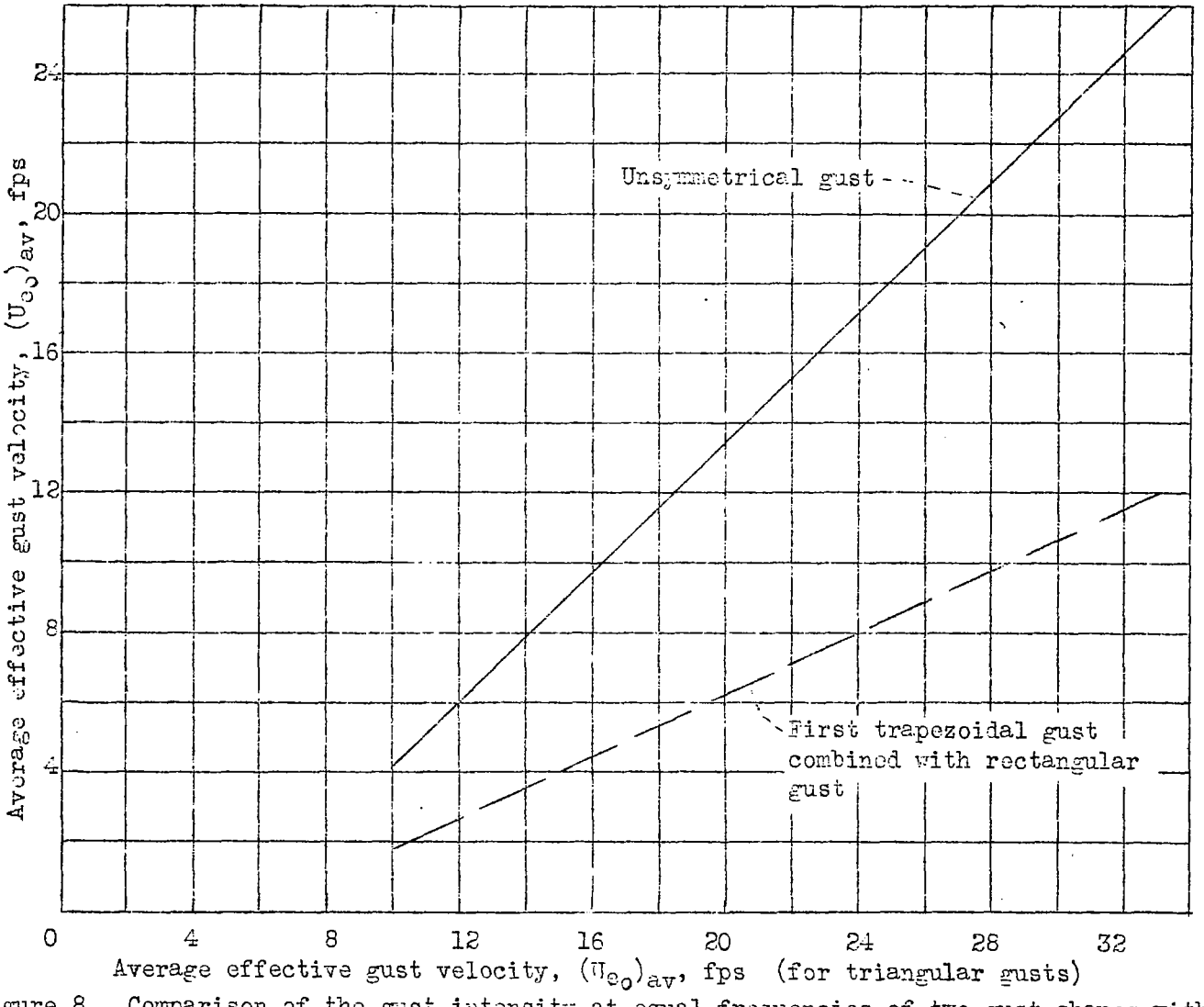

Figure 8.- Comparison of the gust intensity at equal frequencies of two gust shapes with the predominating triangular gust shapes.